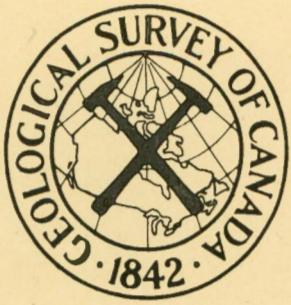

GEOLOGICAL
SURVEY
OF
CANADA

DEPARTMENT OF ENERGY,
MINES AND RESOURCES

PAPER 72-27

FLUVIAL SEDIMENTARY STRUCTURES FORMED EXPERIMENTALLY IN A PIPE, AND THEIR IMPLICATIONS FOR INTERPRETATION OF SUBGLACIAL SEDIMENTARY ENVIRONMENTS

B.C. McDonald
J.S. Vincent

GEOLOGICAL SURVEY
OF CANADA

PAPER 72-27

FLUVIAL SEDIMENTARY STRUCTURES FORMED EXPERIMENTALLY IN A PIPE, AND THEIR IMPLICATIONS FOR INTERPRETATION OF SUBGLACIAL SEDIMENTARY ENVIRONMENTS

(Report and 18 figures)

B.C. McDonald
J.S. Vincent

DEPARTMENT OF ENERGY, MINES AND RESOURCES

Available by mail from *Information Canada*, Ottawa

from the Geological Survey of Canada
601 Booth St., Ottawa

and

Information Canada bookshops in

HALIFAX - 1735 Barrington Street
MONTREAL - 1182 St. Catherine Street West
OTTAWA - 171 Slater Street
TORONTO - 221 Yonge Street
WINNIPEG - 499 Portage Avenue
VANCOUVER - 657 Granville Street

or through your bookseller

Price: $2.00 Catalogue No. M44-72-27

Price subject to change without notice

Information Canada
Ottawa
1972

CONTENTS

Illustrations

ABSTRACT

A series of experiments were performed with a glacio-fluvial sand in transparent acrylic cylindrical pipes of 24.8 and 29.9 cm in diameter, respectively, to gain some insight into sedimentary processes in fluvial systems where water flows beneath ice. One of the objectives was to investigate criteria that might be diagnostic in the field to identify sediments deposited in glacier tunnels flowing full.

With increasing sediment concentration at a given discharge, the sequence of bed forms was: ripple, dune, dune-plane, plane, dune-plane, and total suspension. Dune foresets commonly became finer-grained down the foreslope and displayed a slope discontinuity due to slumping in the upper part of the foreset. Stoss laminations were temporarily preserved due to an upward convexity of the stoss surface. Within the range of experimental variables, dune celerity is directly proportional to the cube of mean flow velocity; the ratio of mean flow velocity to dune celerity is inversely proportional to the square of the Reynolds Number, and symmetry index of the dunes is directly proportional to the square of the Reynolds Number. Dune height is 1/3 to 1 times the hydraulic mean depth. The system tends to maximize the hydraulic mean depth by adjustment of both bed height and bed form.

These relationships are tentatively extended to processes of esker sedimentation with the use of a natural example. Esker sediments deposited in tunnels are characterized by parallel lamination and large-scale cross-stratification, compatible with deposition near maximum hydraulic mean depth. Dune heights indicate actual water depths of 1 to 4 metres, and lead to the suggestion that accumulation of esker sediment was accommodated by a melting upward of the ice roof. Unidirectional flow with high bed-shear was maintained by the ice roof having limited the flow cross-section, and a fluvial sequence was seposited that did not require essentially subaerial conditions.

RÉSUMÉ

Une série d'expériences ont été pratiquées au cours desquelles on a fait circuler du sable d'origine glaciofluviale dans des tuyaux d'acrylique transparents ayant respectivement 24.8 cm et 29.9 cm de diamètre, afin d'étudier l'action des sédiments dans les cours d'eau recouverts de glace. L'un des buts recherchés était d'isoler les caractéristiques qui permettraient d'identifier sur le terrain les types de sédiments déposés dans les conduits de glaciers complètement remplis d'eau.

A mesure qu'augmentait la concentration des sédiments à un point de décharge donné se formaient les accumulations suivantes, dans l'ordre: ride, dune, dune et lit plan, lit plan, dune et lit plan, suspension totale. La granulométrie des fronts de dunes diminuait de haut en bas et la pente subissait une discontinuité due à l'affaissement de la face amont de la dune. La stratification entrecroisée était momentanément conservée en raison de la convexité de la surface stratifiée, en allant vers le haut. A l'intérieur des limites des variables expérimentales, la vitesse de déplacement de la dune est directement proportionnelle au cube de la vitesse moyenne de l'écoulement; le rapport entre celui-ci et la vitesse de déplacement de la dune est en proportion inverse du carré du nombre de Reynolds, et l'indice de symétrie de la dune est en proportion directe du carré de ce nombre. La hauteur de la dune est d'un tiers à une fois la profondeur hydraulique moyenne.

Le système tend à maximiser cette profondeur par l'ajustement de la forme du lit et de sa hauteur.

L'auteur applique ces rapports à la formation des eskers dans la nature. Ces sédiments se déposent dans des tunnels où la stratification est parallèle et qui présentent d'importantes stratifications entrecroisées traduisant une sédimentation qui s'est produite non loin de la profondeur hydraulique moyenne maximale. La hauteur des dunes révèle que la profondeur réelle est d'un à quatre mètres et laisse supposer que la formation des eskers a été facilitée par la fonte de la voûte glaciaire. Un flot en sens unique, avec cisaillement des couches, a été occasionné par le fait que la voûte de glace a limité la coupe de l'écoulement et une séquence fluviale a été déposée, qui n'avait pas nécessairement besoin de conditions subaériennes.

FLUVIAL SEDIMENTARY STRUCTURES FORMED EXPERIMENTALLY IN A PIPE, AND THEIR IMPLICATIONS FOR INTERPRETATION OF SUBGLACIAL SEDIMENTARY ENVIRONMENTS

INTRODUCTION

In numerous localities where Wisconsin ice fronts retreated down the regional topographic gradient, for example throughout southern Quebec and the Hudson Bay Lowlands, a deep-water environment was ponded against the ice front and expanded northward in contact with the retreating glacier front. In areas such as the District of Keewatin west of Hudson Bay, the eustatically rising sea abutted the retreating ice front.

The standard stratigraphy in these areas would be till directly overlain by silt and clay deposited in quiet water. Commonly in these areas, however, till is separated from overlying silt and clay by sequences of cross-bedded sand and coarse gravel that resemble normal fluvial successions. Sets of cross-strata are typically less than 40 cm thick, although sets thicker than one metre have been observed. These sequences are locally as thick as 30 metres and can take the form either of relatively broad sheets or of linear accumulations of esker sediment.

The problem, then, is to explain how a thick sedimentary sequence containing evidence of high bed-shear stress and resembling a normal fluvial succession can be deposited near an ice front at a depth far below the level of the water body in contact with the glacier terminus. One possibility is that unidirectional flow with a high bed-shear stress could have been maintained by the presence of an ice "lid" having reduced the flow cross-section through which basal meltwater had to discharge.

Some eskers, including one that the senior author has studied in detail, are believed to have been deposited in subglacial tunnels that debouched into a deep water body at the glacier terminus. Subglacial tunnels flowing full are gigantic natural pipes in which bed forms that depend on surface water waves cannot be stable. It would be expected, then, that sedimentary structures derived from antidunes would be absent. If it were possible to characterize further a subglacial fluvial sedimentation environment from the structural or textural characteristics of the sediment, the criteria could be applied to the interpretation of near-glacial sedimentary environments. Perhaps river sediments deposited under a winter ice cover could also be identified as such in the geologic record.

A simple pipe-flow experiment was designed that would permit observation of bed forms and sedimentary textures and structures through transparent pipe walls under a variety of pipe-flow conditions. In addition to study of sedimentary textures and structures, an attempt was made to determine whether safe inferences could be made concerning depth and velocity of the paleo flow system.

Original manuscript submitted: 23 December 1971
Final version approved for publication: 26 April 1972

Acknowledgments

The authors would like to acknowledge the capable laboratory assistance of D. L. Forbes and D. M. Morel. The manuscript has benefitted materially from critical examination by D. L. Forbes and Dr. W. H. Mathews.

APPARATUS

The experiments were performed in the return-pipe section of the tiltable, recirculating, sedimentation flume of the Geological Survey of Canada (Fig. 1; McDonald, 1972). In this flume, water and sediment leaving the main open channel fall into a tank from which the mixture is pumped back to a headbox via two return pipes of circular cross-section, 24.8 cm and 29.9 cm inside diameters, respectively. The proportion of the discharge that passes through each pipe is controlled by a valve system. Because the pipes carry flow up to the flume headbox, all sediment transport in the pipes was up an adverse slope.

In the straight section of each return pipe, immediately downstream from a 45 degree elbow, is mounted a 5-metre length of smooth, transparent, acrylic pipe of the same inside diameter as the rest of the pipe system. The transparent sections permit examination of the sediment transport processes, and these can be related to conditions in the flow system. A limitation of the apparatus is that the bed can be observed but not directly sampled.

The discharge through each pipe, Q, is measured with the aid of a side-contracted, sharp-edged orifice plate mounted in the pipe. The orifice plate generates a pressure differential which is a calibrated function of the flow rate through the pipe. Plastic tubes lead from each side of the orifice plate to a differential mercury-water manometer where the discharge can be read.

Measurements of the bed forms in the pipes were made during and after each run. Measurements of the system during the runs were made at the downstream end of the transparent sections, where turbulence generated by the elbow bend would have least influence on the bed. A template that fitted the outside of the pipe was used to measure heights of the bed forms, H; lengths λ, were measured with a graduated tape. Bed-form celerities (i.e. the velocities of their forward migration), were monitored with a stopwatch.

Total concentration of sediment in transport, C_T, was sampled at the downstream end of the open channel after the entire system had reached equilibrium. The criterion for equilibrium was the existence of uniform flow in the open channel. Precision of sediment concentration values was dependent on the equilibrium bed form in the open-channel part of the system. Sampling time varied from two to five minutes, depending on the discharge, and variations in C_T depended on whether or not a voluminous bed form was migrating out of the channel during the sampling interval. Approximate variations from the average values, based on two to four samples collected while the system was in equilibrium were: for $C_T < 100$ ppm, $\pm$ 80%; $2,000 > C_T > 100$, $\pm$ 25%; for $C_T > 2,000$, $\pm$ 10%.

Measurements of mean bed height were converted from tables in Chow (1959) to give the cross-sectional area carrying the flow. This was divided into discharge to give mean flow velocity, V.

Head-loss measurements were not taken along the pipe system, hence slope of the energy grade line is not known.

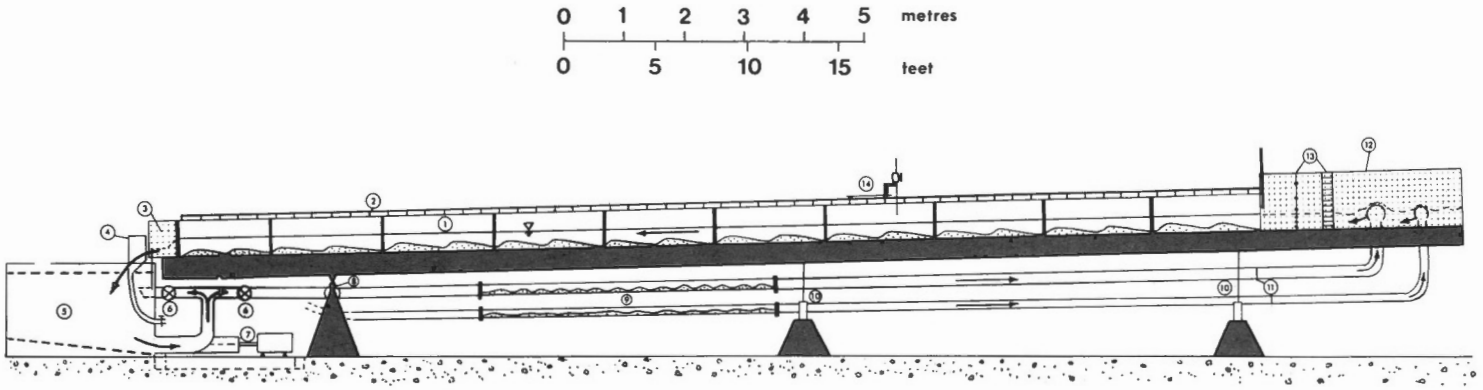

1. main channel
2. rails
3. tailgate assembly
4. total lead sampler
5. tail tank
6. flow-control valves
7. pump and motor (small pump, not shown, feeds the 25 cm return pipe)
8. pivot support
9. transparent sections of return pipe
10. jack supports
11. orifice plates
12. headbox
13. baffles
14. instrument carriage

Figure 1. Generalized longitudinal diagram of flume. GSC photo 201787

EXPERIMENTS

Previous Work

Because of the industrial applications of pipe transportation of clastics to such fields as waste disposal, dredging, and conveyance of ores and other materials within industrial plants, engineers have provided an extensive body of experimental data on sediment movement in pipes (cf. Graf, 1971, Chap. 15; Task Committee, 1970). Generally, however, these studies have concentrated on considerations of head loss and power requirements.

Four modes of transport of solid-liquid mixtures through pipelines have been recognized by engineers (cf. Task Committee, 1970, p. 1504). The boundaries between these modes of transport are shown qualitatively on Figure 2(a), along with actual points corresponding to experimental runs reported in the present study. In general, as velocity is increased particles begin to move and the "stationary" bed (mode I) is transformed into a moving bed (mode II) on which grains move by sliding, rolling, and saltating. It is this mode that sustains bed forms. With continued increase in velocity, all the sediment goes into suspension; first the sediment concentration is greatest near the pipe floor (mode III), but at higher velocities the suspension is increasingly homogeneous (mode IV). In mode III the amount of material transported per unit of power consumption is at a maximum (Task Committee, 1970). Acaroglu and Graf (1969) have noted that the rate of consumption of energy increases more or less constantly with increasing mean velocity except in the plane-bed mode where increasing velocity is not accompanied by appreciable increase in the slope of the energy grade line.

A sediment bed in the pipe is undesirable in industrial application because of the friction losses that result. Consequently, few experiments have been conducted with natural sediments and a mobile bed in transparent large-diameter pipes. Few studies report details of bed-form characteristics and the present authors are aware of none that report on sedimentary structures.

In experiments with very coarse sand and granules in a 7.6-cm-diameter pipe system containing a 1.85-metre transparent observation section, Acaroglu and Graf (1968) reported the following succession of bed forms as bed-shear stress was slowly increased over an initial stationary horizontal sediment bed: (1) "critical condition" with a few grains in motion but no new bed form; (2) dunes; with increasing flow intensity they lengthened and showed increasing tendency for grains to be moved in saltation; (3) plane bed (i.e., a bed without any irregularity larger than a few particle diameters) with grain movement both as bed load and suspended load; (4) "sliding bed" where the whole bed, while essentially maintaining a planar surface, moved slowly and intermittently although most sediment transport was by suspension; and (5) heterogeneous suspension. They found that the inter relationships of flow characteristics and bed forms in pipes were basically similar to those in open channels except that a "sliding bed" mode in the pipe, although not observed by other workers, seemed to occur instead of antidunes at higher flow intensities.

In experiments with an 18-metre lucite pipe 14 cm in diameter, Craven (1952) found that as concentration of sediment in transport was increased, all other parameters being held constant, isolated dunes appeared. The spacing between dunes decreased until the dunes merged, then lengthened and flattened until the bed became perfectly plain. He also found that values of sediment concentration at the transition from dune to plane bed depended on the

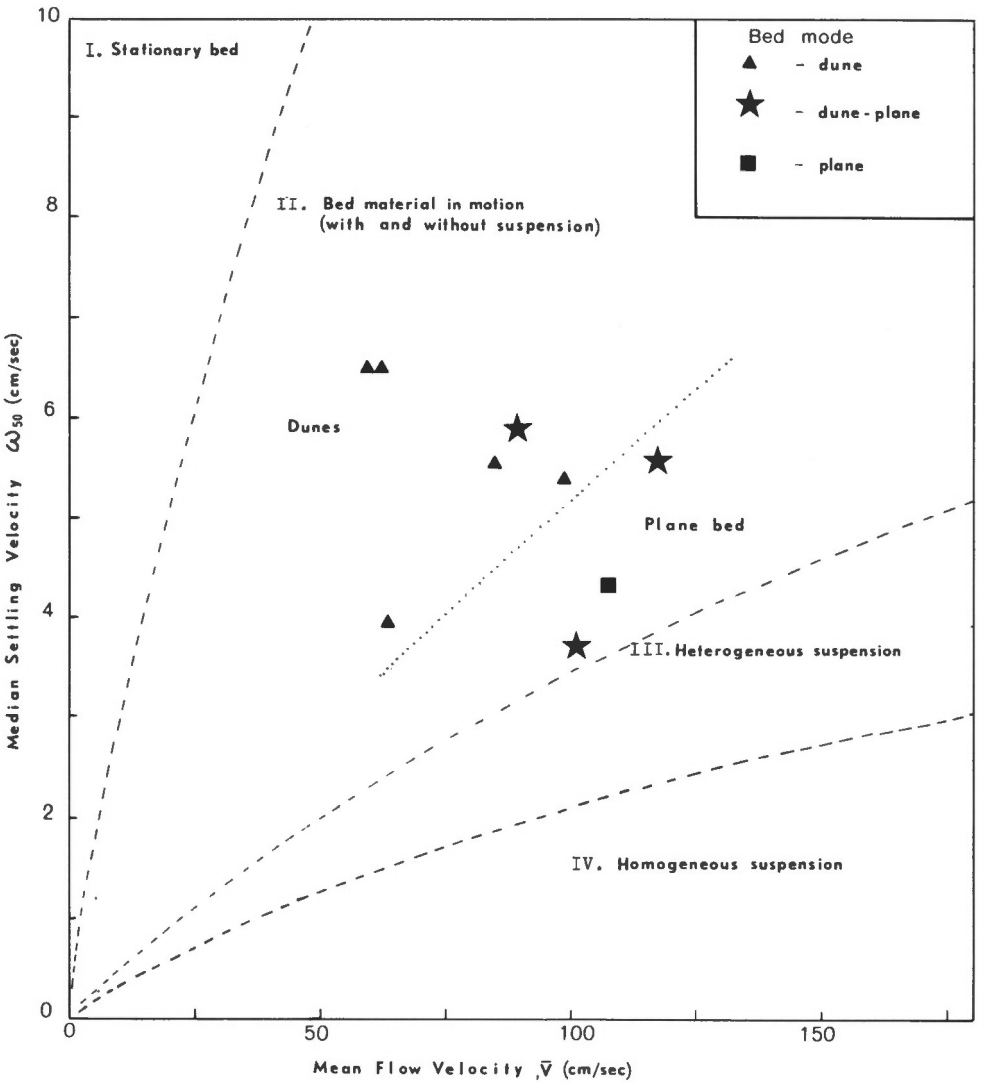

Figure 2(a). Generalized modes of sediment transport in pipes; experimental data plotted apply to transport in 24.8-cm pipe with sand used in present experiment, and with $\bar{C}_T > 100$ ppm.

grain size of the sediment in transport. Under these conditions, the implications of sediment concentration for such indices of bed-form shape as ripple index and ripple symmetry index are clear. However, bed profiles (Craven, 1952, his Figs. 4 and 5) indicate an aggrading bed in the pipe as the bed form changed. This would change the hydraulic mean depth and affect the shear stress on the bed. It cannot be determined from the report whether or not these parameters were kept strictly invariable.

Present Experiments

The present observations were made during sixteen experimental runs (22 through 37) that were being carried out primarily to study phenomena in the open-channel part of the apparatus. By partitioning the discharge between the 24.8 cm and 29.9 cm return pipes, a total of 13 sets of data were obtained for the 24.8 cm system and 6 sets for the 29.9 cm system. For the 24.8 cm pipe, an attempt was made to obtain several sets of data at the same discharges, so the effect of sediment concentration could be determined.

Duration of continuous runs varied between 6.3 and 70.5 hours, depending upon attainment of equilibrium in the system. The measurements were taken over several hours while the system was in equilibrium. Generally, the bed forms were regular over at least the downstream 2.5 metres of transparent pipe section, indicating negligible effect of the elbow that was located immediately upstream of the acrylic pipe. In run 31A, however, well-defined dunes appeared only in the last metre or so of pipe, with a plane bed upstream of this.

The sand used in the experiment was a glaciofluvial sand from the Ottawa area, Ontario. Median sieve diameter is 0.47 mm; phi derivation is 1.24; median settling velocity, ω_{50}, through calm water is 6.50 cm/sec. Cumulative settling velocity and grain-size curves are shown in Figure 3. Comparison of sieve diameter and settling velocity indicates a Corey shape factor $\left(\frac{c}{\sqrt{ab}}\right)$ equal to 0.55 (U.S. Inter-Agency Comm. on Water Resources, 1958, p. 36).

Present experimental data (Table I) have been plotted on Figure 2(a) in such a way as to illustrate the interrelationship of the four modes of sediment transport. Mode II, i.e. flow with a moving bed (including saltation), is the environment of most interest to sedimentologists and the one containing most of the present experimental data. However, it can be seen from Figure 2(b) that the stable bed form is dependent also on concentration of sediment in transport, $\bar{C}_T$. Increasing values of V/ω_{50} would be accompanied by an increasing tendency for sediment to be transported in suspension. The importance of this relationship for sedimentary structures would be that development of a plane bed, thereby producing a sediment with parallel lamination, would be favoured by relative decrease of ω_{50} or by relative increase of either $\bar{V}$ or $\bar{C}_T$ in the system.

In runs 24, 28, and 33 both pipes were used concurrently in order to provide sufficient discharge for the open-channel experiment while keeping velocities low enough in the pipes to permit existence of a bed. Two problems are posed by this arrangement. There is no way to directly sample the concentration of sediment in transport in each pipe. The concentration measured for the system can be applied, with reservation, to each pipe. Also, particularly in run 33, sediment appeared to be sorted somewhat in the end tank; the bed in the 24.8-cm pipe appeared to be finer grained and contain a higher proportion of heavy minerals than the bed in the 29.9-cm pipe.

In runs 26A, 30A, 32A, and 34A the concentration of sediment in transport was less than 75 ppm by weight. The bed record for these runs is particularly inconclusive and the results have not been plotted on the graphs that follow. In runs 26A and 30A a discontinuous disperse layer of sediment one grain thick was observed sliding and rolling along the pipe floor. The only apparent organization of grains was a lateral variation in grain concentration that was probably related to downstream movement of turbulent eddies.

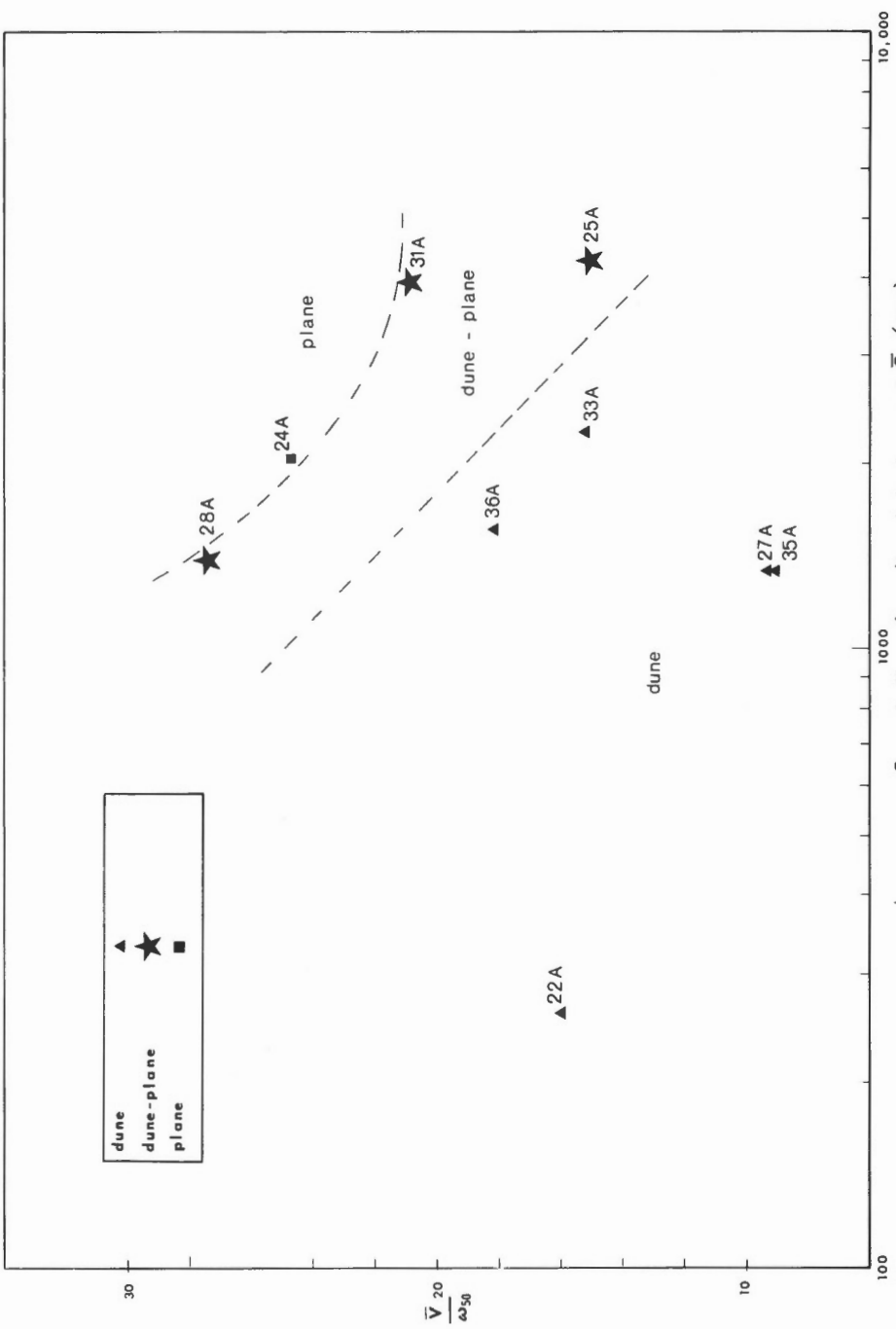

Figure 2(b). Relationship of stable bed form to $\overline{V}$, ω_{50}, and $\overline{C}_T$ in 24.8-cm pipe.

Table I – Experimental data

Runs			Hydraulic Parameters							Average bed-form measurements						
Run no.; pipe size (A=24.8cm; B=29.9cm)		Duration (hrs.)	Adverse slope of pipe	T (° C)	Q (l/sec)	$\bar{V}$ (cm/sec)	$\bar{C}_T$ (ppm)	w_{50} (cm/sec)	R (cm)	Re x10^3	No. forms measured	$\bar{H}$ (cm)	$\bar{\lambda}$ (cm)	$\overline{RI}$	$\overline{RSI}$	$\bar{c}$ (cm/sec)	Bed mode (*occasionally starved bed)
24.8 cm pipe	22A	48	.0061	28.8	30.0	63.3	259	3.95	7.10	219	25	2.4	35	15.6	5.3	0.38	dune*
	24A	48	.0045	26.4	45.0	106.2	2,014[a]	4.30	7.55	369	-	-	-	-	-	-	plane
	25A	38	.0085	28.6	30.0	88.7	4,247	5.90	7.19	310	38	6.2	146	23.8	13.4	0.87	dune-plane
	26A	61	.0089	26.1	30.0	62.1	23	4.60	6.20	202	-	-	-	-	-	-	single-grain layer
	27A	47	.0059	26.0	20.7	60.2	1,332	6.50	7.23	199	9	6.5	96	15.3	7.2	0.25	dune
	28A	37	.0065	26.0	41.6	101.6	1,388[a]	3.70	7.54	350	2	5.2	72	-	7.8	-	dune*-plane
	30A	70	.0048	28.3	30.0	62.1	63	5.90	6.20	185	-	-	-	-	-	-	single-grain layer
	31A	6	.0114	25.2	36.8	117.0	3,918	5.60	6.99	367	4	4.7	70	16.2	16.5	0.86	dune-plane
	32A	46	.0054	25.1	44.0	91.1	52	6.00	6.20	252	-	-	-	-	-	-	no bed
	33A	37	.0091	24.0	30.0	84.4	2,266[a]	5.55	7.32	269	14	6.4	114	18.1	10.1	0.44	dune*
	34A	48	.0052	26.5	22.1	46.0	56	6.20	6.78	144	4	0.8	66	92.5	ca.3	0.06	low dune
	35A	35	.0066	26.1	22.6	59.0	1,380	6.50	7.45	201	24	6.3	82	13.4	7.2	0.29	dune
	36A	3x13[b]	.0068	26.5	43.5	98.4	1,552	5.40	7.50	341	18	4.0	71	18.3	18.6	0.92	dune*
29.9 cm pipe	23B	38	.0044	26.0	60.0	89.4	2,166	4.12	8.86	361	42	5.5	82	15.9	9.1	0.87	dune*
	24B	48	.0034	26.4	45.0	73.0	2,014[a]	4.30	9.10	306	26	7.1	88	12.4	8.0	0.43	dune*
	28B	37	.0054	26.0	40.0	66.4	1,388[a]	3.70	9.10	276	13	5.2	67	15.5	6.9	0.48	dune*
	29B	70	.0063	28.6	51.0	73.0	280[a]	4.30	8.18	289	12	1.0	96	87.9	16.5	0.73	dune*-plane
	33B	3x37	.0080	24.0	57.0	87.9	2,266[a]	5.55	9.02	345	10	4.9	91	20.2	9.9	0.89	dune*-plane
	37B	6.5[b]	.0090	22.5	65.6	103.1	2,543	5.40	9.07	393	3	3.7	117	31.5	13.4	0.71	dune-plane

a. Both pipes used concurrently; same $\bar{C}_T$ and w_{50} values are applied to both in table.

b. Runs 36A and 37B interrupted twice.

Velocity of large rolling grains was one third to one half the mean flow velocity. In run 30A some grains had short rest periods of about one second, indicating a nearness to true bed development. In run 32A all grains were in suspension. Low, smooth-crested bed forms, less than about 1 cm high, were observed occasionally during run 34A. These may have been incipient dunes, although their low celerity (0.06 cm/sec.; Table I) suggests similarity to the undulating bed form reported from run 29B.

Occasionally the bare pipe floor was exposed downstream from dune foreslopes, particularly in the zone of excessive turbulence and erosion where flow lines that had separated from the bed at the dune crest were reattached to the bed. Such dunes were termed 'starved'. Runs in which dunes were occasionally starved are marked in Table I.

Where the stable bed configuration varied between dunes and plane bed (runs 25A, 28A, 31A, 33B, and 37B), bed measurements for the dunes are reported in Table I.

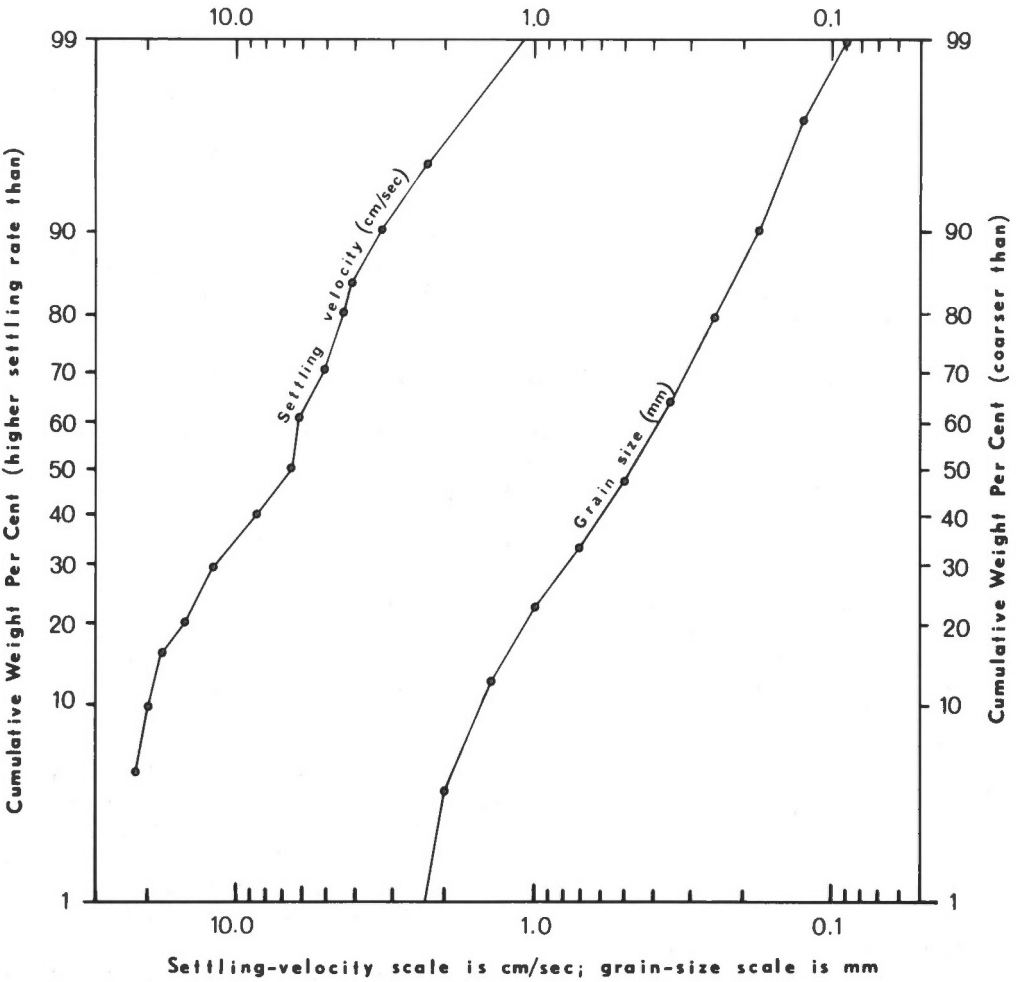

Figure 3. Distribution of grain sizes and settling velocities in a bulk sample of the sand used.

DISCUSSION OF RESULTS

Bed Forms and Sedimentary Structures

Although small ripples have been formed with this particular sand in the pipes, discharge associated with the ripples was too low to measure accurately with the manometer. Only the dune, plane bed, and no-bed modes were stable in the runs reported here.

Dune mode

In most runs, dunes were the stable bed forms. Features of dune shape, stratification, and sorting that were commonly observed in the pipe are illustrated in Figure 4. As with open-channel systems, dunes migrated forward by material rolling, sliding, and saltating up the stoss side and being deposited on the foreslope in the zone of flow separation immediately downstream from the crest. The turbulence resulting from reattachment of the flow to the next stoss slope downstream from a dune front was a major influence in bed erosion and in the entrainment of large quantities of material into suspension. Figure 5 shows a characteristically dense saltation carpet in motion across a dune, and the dense cloud of sediment immediately downstream of the crest where the rolling carpet is in suspension momentarily before settling onto the foreslope. Foreset laminae were tangential at the base.

The zone of back flow occupied about the lower one-third of the zone of flow separation in the lee of the dune crests. Grains settling through the zone of flow separation were thrown sharply back onto the foreslope when they encountered the back eddy.

Several characteristics of the dunes were noted which may occur more frequently in pipes than in open channels and, therefore, may prove useful as field criteria:

(a) Foresets of pipe-flow dunes commonly showed a decrease in grain size down the foreslope. This textural change was readily visible in cross-section (Figs. 6,7), where the uppermost one-third of the foreset laminae was noticeably coarser grained than the lower two-thirds. This feature is thought to be due to deformation of the zone of flow separation by the pressure resulting from suppression by the pipe of the out-of-phase surface water wave normally associated with dunes in open channels. The zone of flow separation would be crowded closer to the foreslope. Fine-grained material formerly in saltation and low suspension could settle through the zone of flow separation and be thrown onto the lower foreslope by the back eddy before coarser bed material, formerly in traction, could avalanche to lower portions of the foreslope.

(b) The thick carpet of bed material in transport caused frequent "over-building" of the upper part of the foreslope, followed by slumping to a lower angle of repose and avalanching of material part way down the foreslope. This slumping mechanism, which occasionally involved a layer 1 cm thick on the foreslope, resulted in the preservation of a recognizable slope discontinuity near the upper end of the foreset lamination (Figs. 4, 6, 7). The oversteepened upper foreslope is visible in Figure 5.

(c) Stoss sides tended to be convex-up, with the top of the foreslope notably lower than portions of the stoss side (Figs. 4, 5). This resulted in the occurrence of stoss laminae, parallel and relatively fine grained, as

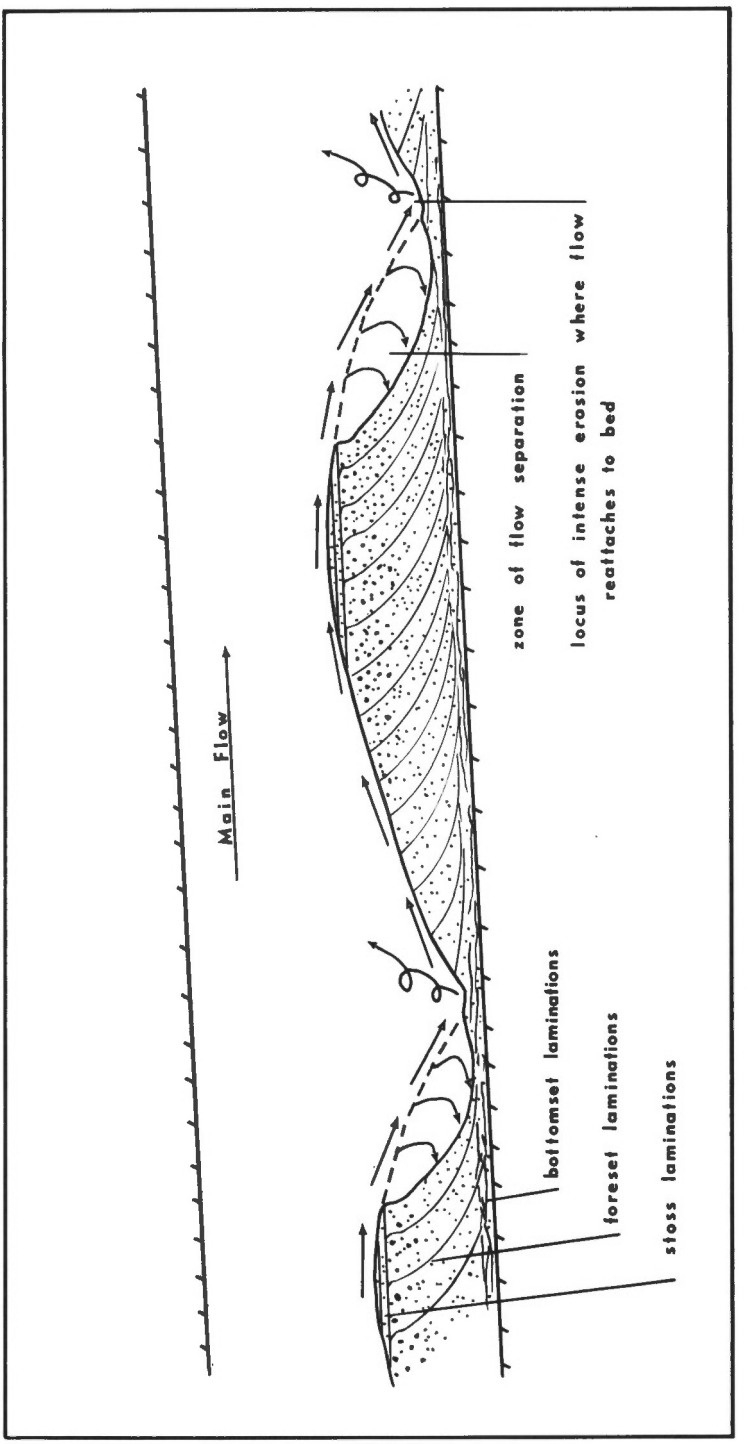

Figure 4. Generalized characteristics of dune shape, stratification, and sorting as exposed through transparent pipe walls.

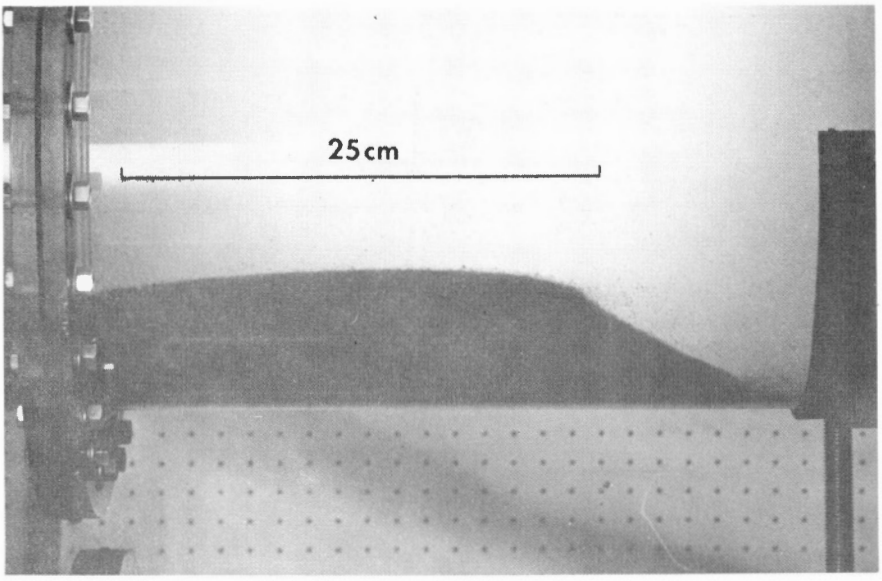

Figure 5. Dune building forward during run 28B. Note grains moving in saltation, and cloud of temporarily suspended sediment downstream from crest. Also visible are convex-up stoss side and small slope discontinuity in upper part of foreslope. (GSC photo 159718)

thick as 1 cm on the dune. Widespread field preservation of these laminae would permit direct field measurement of full dune height.

Deposition of a dune sequence in the pipes produced a cut-and-fill succession of large-scale cross-stratification (Fig. 8) which was similar to a sub-aerially formed fluvial succession, excluding differences in structure and texture already mentioned. Such a relatively complex succession is due, in large part, to variable rate of forward migration, or celerity, c, of adjacent dunes. As with open-channel systems, variable dune celerities resulted in faster dunes overtaking slower ones. As the faster dune approached, more and more of the bed material that formerly supplied the foreslope of the slower dune was stored in the faster dune. This resulted in progressive atrophy of the leading slower dune until the faster 'parasite' reached the crest of the slower dune. Then forward migration of the new, single, larger dune began. Figure 9 shows a dune complex where the faster dune has migrated up the stoss side almost to the crest of the leading shower dune.

Celerities of stable dunes varied between 0.25 and 0.92 cm/sec. Figure 10(a) shows that, within the range of flow velocities tested, average dune celerity is related to the cube of mean flow velocity by the approximate relationship:

$$\overline{c} = \frac{\overline{V}^3}{10^6}$$

In a study with spherical glass beads in transparent pipes less than 10 cm in diameter, Thomas (1964) formed dunes and reported that celerity varied as the

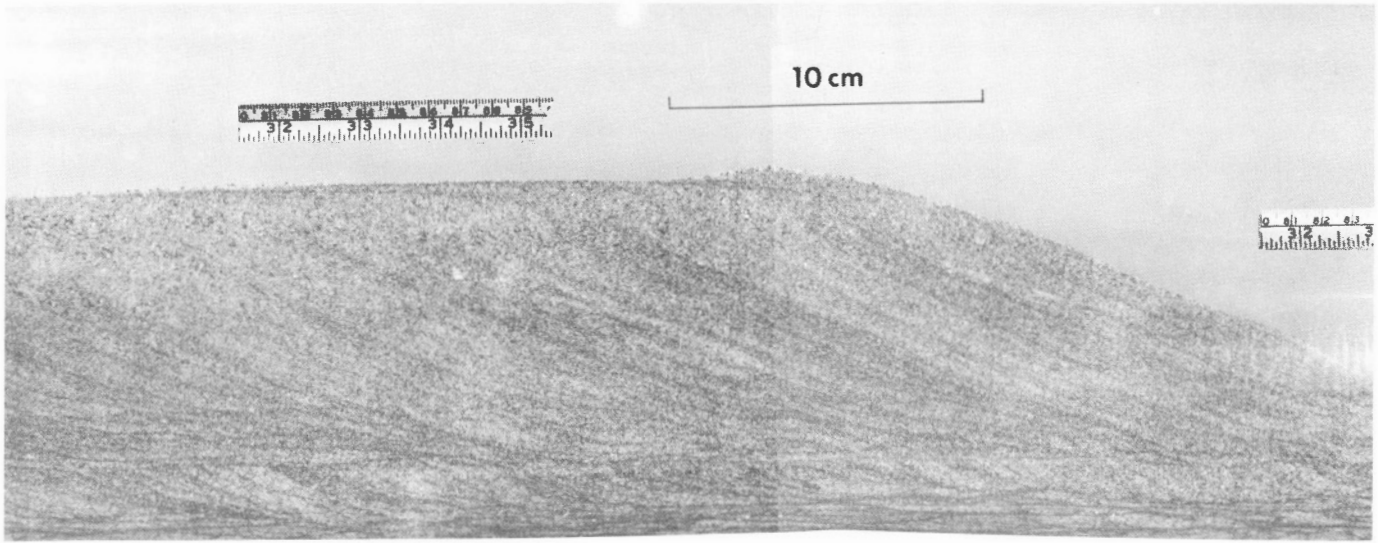

Figure 6. Dune in pipe after run 33A. Note gradation from coarse to fine down the foreset laminations; base of foresets tangential; slope discontinuity in upper part of some foresets; and thin stoss laminations. Small deposit 0.6 cm thick on crest was formed by backflow up foreslope when flow was stopped suddenly. Scale on photo in centimetres and inches.
(GSC photos 159723 and 159722)

fifth power of mean flow velocity. The relationship between flow velocity and celerity could be useful in assessing sedimentation rates in an aggrading system where an independent measure of mean flow velocity was available. Figure 10(b) indicates that hydraulic mean depth (R), through Reynolds Number (Re), influences the ratio of mean flow velocity to dune celerity according to the relationship.

$$\frac{\overline{V}}{\overline{c}} = \frac{12.5 \times 10^{12}}{Re^2}$$

As viscosity and mean flow velocity remain constant, increased hydraulic mean depth is accompanied by an increase in dune celerity.

Bed-form shape indices are commonly used as environmental indicators (e.g. Tanner, 1967). "Ripple index" (ratio of bed form length to height) and "ripple symmetry index" (ratio of length of stoss side to length of lee side) were measured (Table I), and attempts were made to relate the values to various flow parameters. Figure 11 indicates the variability of dune height (H), dune length (λ), ripple index (RI), and ripple symmetry index (RSI) among the more than forty measurements made at equilibrium during run 23B.

Ripple indices in run 23B (Fig. 11) had a skewed distribution and varied between 6.8 and 32.0 with a mean of 15.9. With the exception of two particularly high values, average ripple indices for the runs varied from 12.4 to 31.5. The value of 92.5 in run 34A was associated with a sediment concentration of only 56 ppm which may explain the low bed-form height and hence the high ripple index. The value of 87.9 in run 29B was associated with washed out dunes near the dune-plane bed transition. There was no well-defined zone

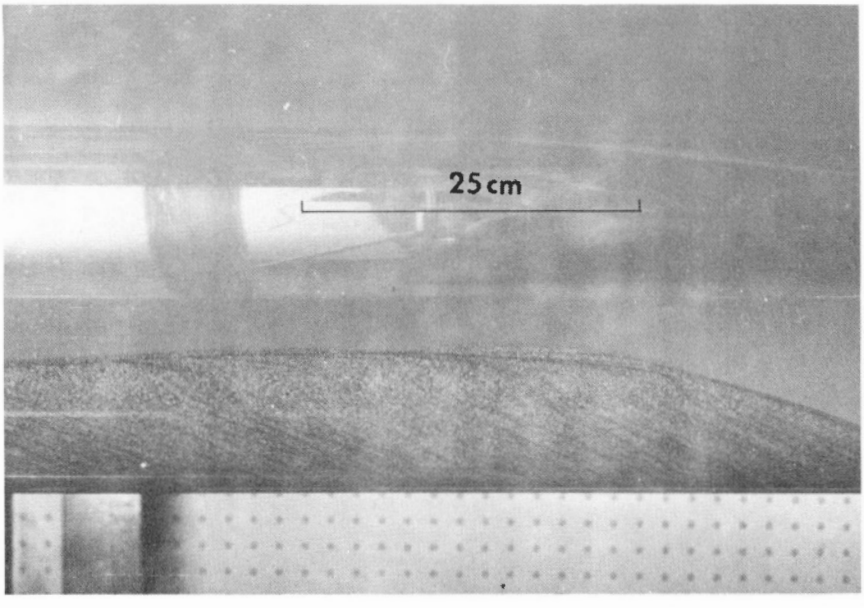

Figure 7. Dune in pipe after run 24B. Note gradation from coarse to fine down the foreset laminations, and the slope discontinuity in the upper parts of the foresets. (GSC photo 159717).

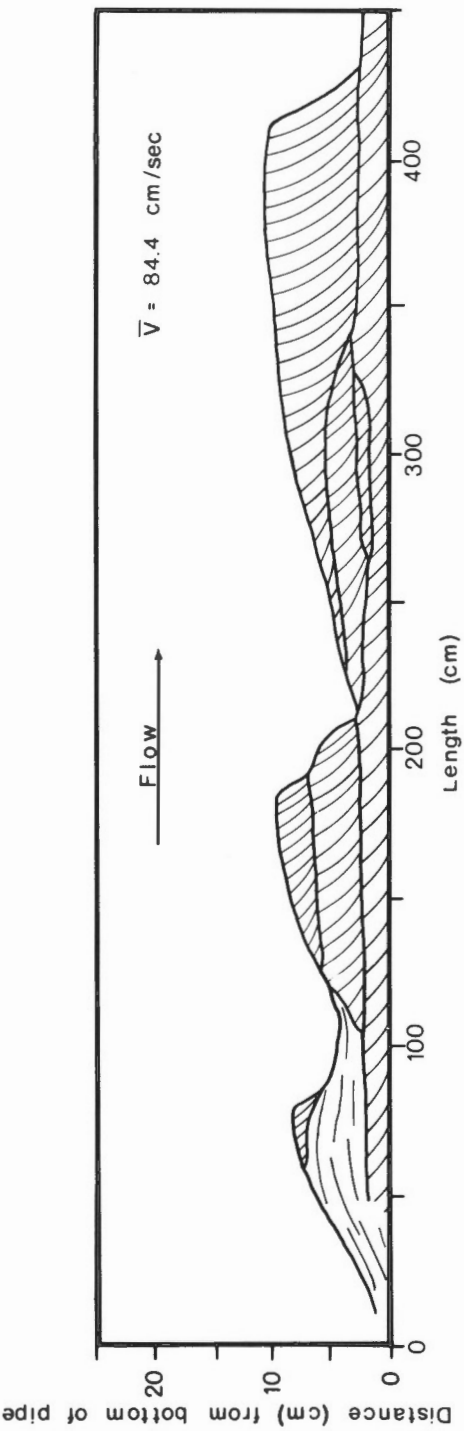

Figure 8. Diagram of dunes and stratigraphy, run 33A. (Fig. 6 from station near 400 cm, and Fig. 9 from station near 175 cm).

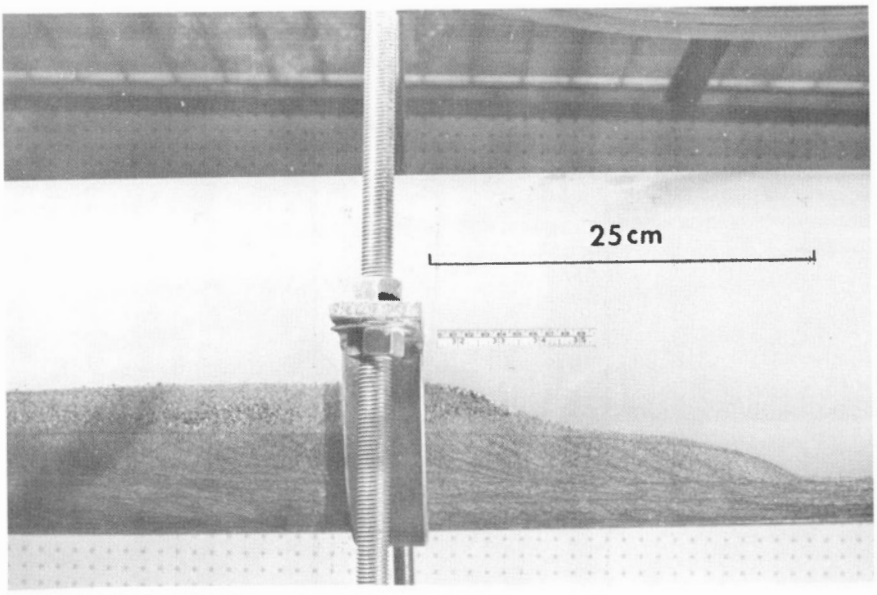

Figure 9. Dune complex resulting from variable dune celerities, run 33A. Scale in photo in centimetres and inches. (GSC photo 159724)

of separation downstream from the smooth crest, and the bed was underlain by gently dipping parallel lamination. Thomas (1964) reported experimental values of ripple indices from 9 to 40. No clear relationship could be found in the present experiment between ripple index and any of the hydraulic parameters.

Ripple symmetry index varied in run 23B between 1.4 and 18.1, with a mean value of 9.1. Average values for the runs varied between about 3 (run 34A) and 18.6. There is a tendency for RSI values to increase with increasing $\overline{C}_T$. Mean flow velocity and hydraulic mean depth are related, through the square of the Reynolds Number, to ripple symmetry index (Fig. 12) according to

$$RSI = \frac{1.15\ Re^2}{10^{10}}$$

An increase in either $\overline{V}$ or R will lengthen the stoss side relative to the lee side. It is evident from Figure 10(b) that ripple symmetry index increases with an increase of dune celerity relative to mean flow velocity, according to

$$RSI = \frac{1440\ \overline{c}}{\overline{V}}$$

and that, for this sand in this experiment

$$RSI = .00144\ \overline{V}^2, \text{ and}$$
$$RSI = 14.4\ \overline{c}^{2/3}$$

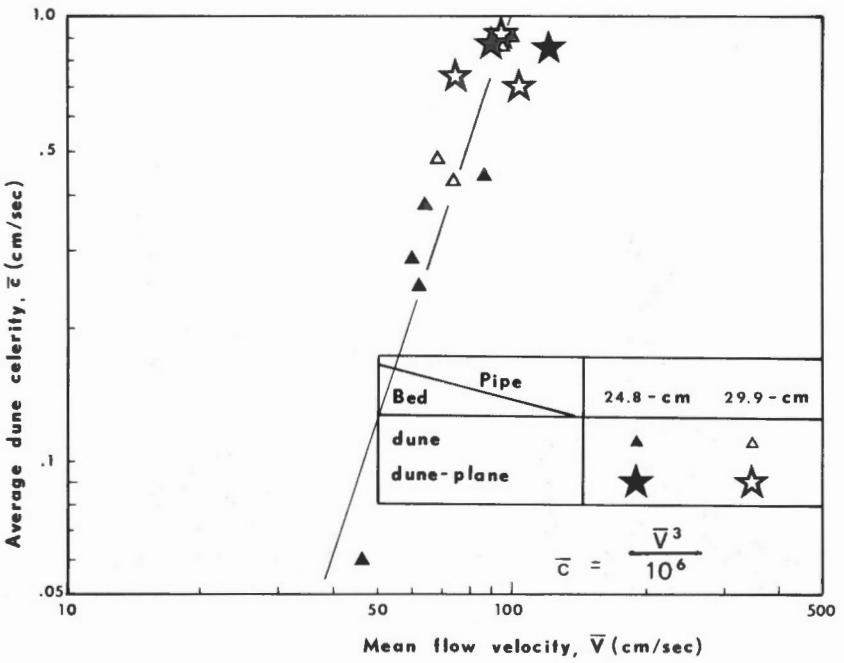

Figure 10(a). Relationship of average dune celerity to mean flow velocity.

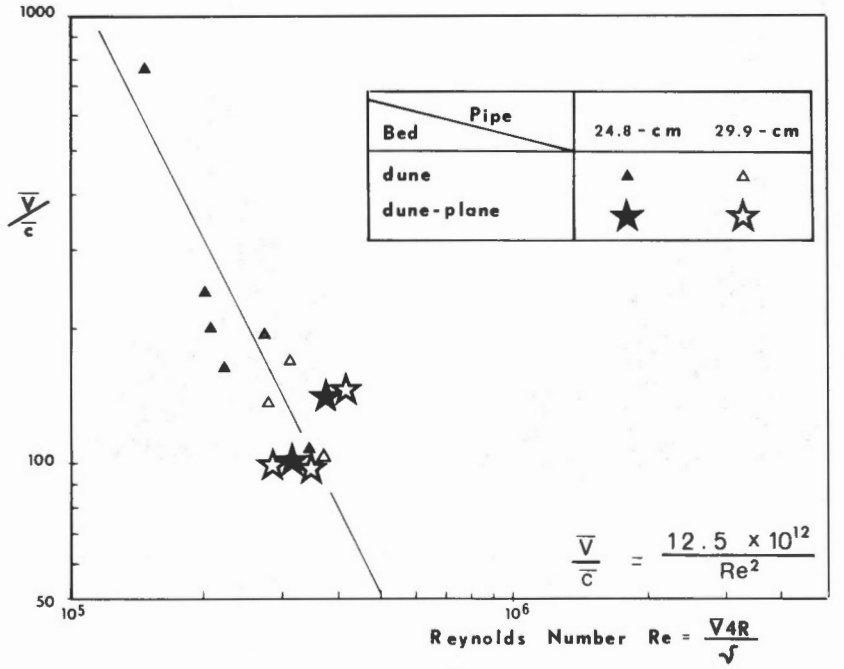

Figure 10(b). Relationship of $\overline{V}/\overline{c}$ to Reynolds Number.

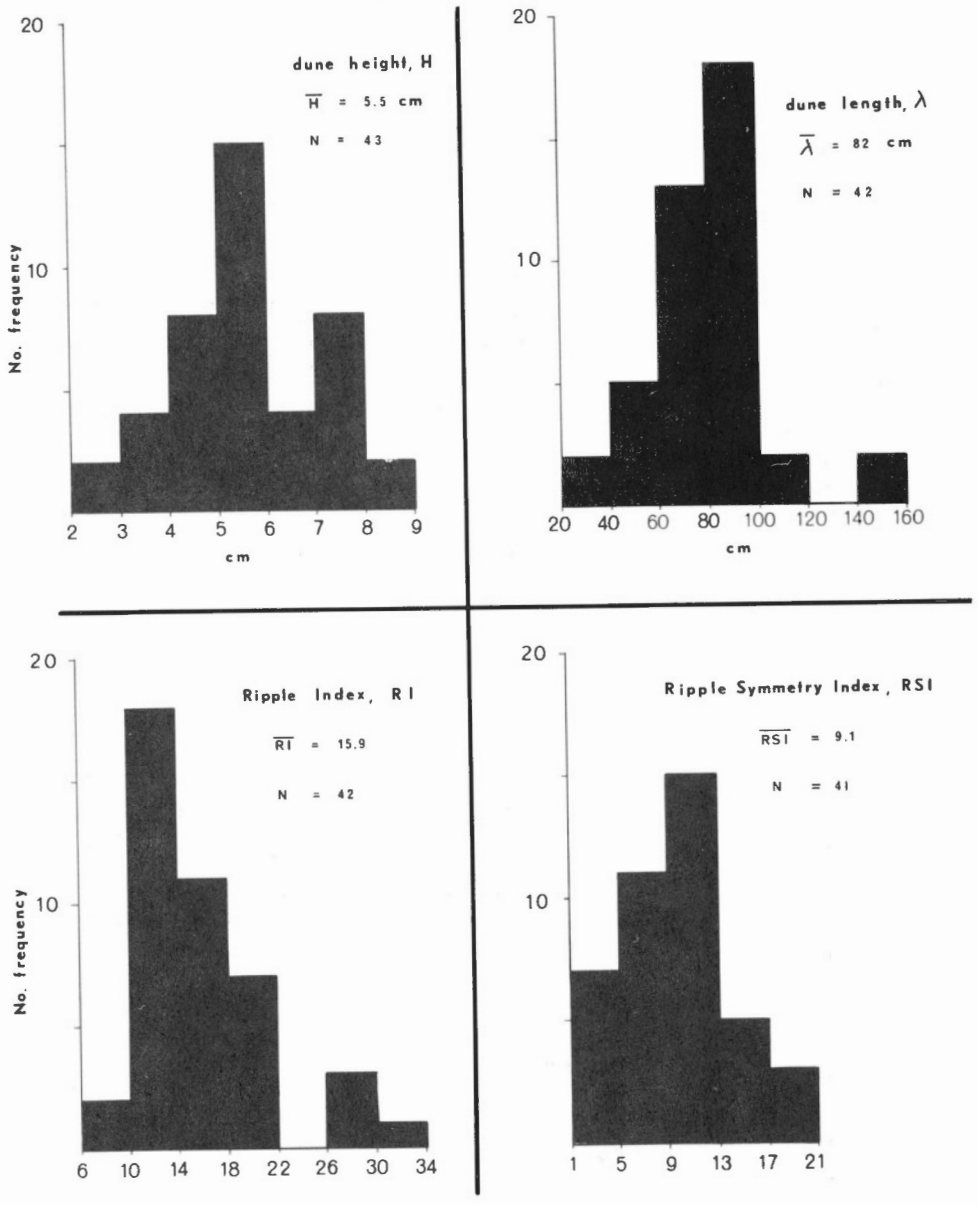

Figure 11. Variability of dune measurements and shape indices under equilibrium conditions during run 23B.

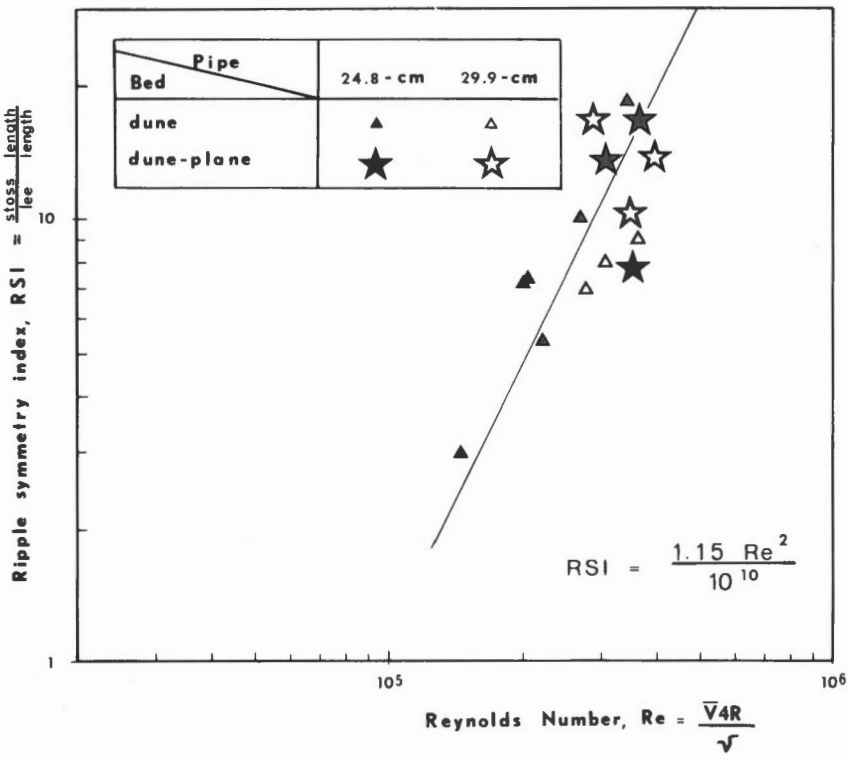

Figure 12. Relationship of Ripple Symmetry Index to Reynolds Number.

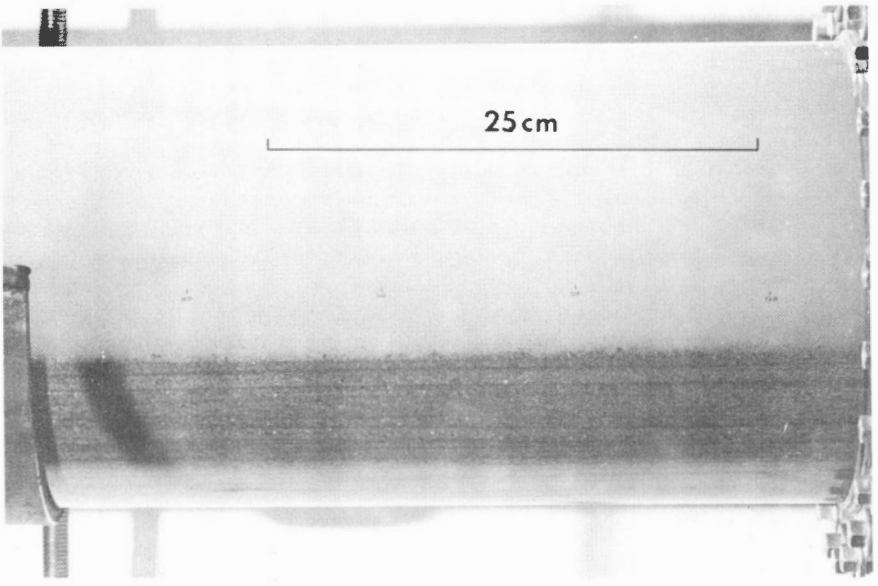

Figure 13. High concentration of suspended sediment near bed during run 31A; parallel laminations underlie plane bed. (GSC photo 159720)

Dune-plane bed transition and plane bed

At higher values of $\overline{C}_T$ or $\overline{V}$, or at lower values of ω_{50}, the bed tended to be plane with a high concentration of suspended sediment near the bed (Fig. 13).

The threshold between dune and plane-bed modes is very delicate. In run 25A, for example, excessive local turbulence would trigger an instability that would almost instantaneously transform a plane-bed regime into a bed of large dunes. This instability is related to local entrainment and displacement of such a large volume of sediment that lee-side separation would occur and the accompanying turbulence would spawn a new dune train downstream of the initial scour. Minutes later the bed would be plane again. The transition was observed in runs 25A, 28A, 31A, 29B, 33B, and 37B (Table I). This transition took place at Froude Numbers between 0.82 and 1.41, where

$$\text{Froude Number } Fr = \frac{\overline{V}}{\sqrt{gR}}$$

It is also probable that fluctuations of $\overline{C}_T$ associated with dunes leaving the open-channel influenced the fluctuation between dune and plane-bed modes in the pipe (dunes were present in the open-channel part of the apparatus in runs 28A, 29B, and 33B). Higher concentrations of sediment in transport would favour development of a plane bed (Fig. 2(b); Craven, 1952). A stable plane bed was observed only in run 24A.

In runs 28A, 34A, and 29B, dune-like bed waves formed that appeared transitional with a plane bed in that the bed waves were low, smoothly convex-up, and showed almost no flow separation downstream from the poorly defined crest. The bed-form indices and celerity reported for run 34A in Table I are for forms of this type. Celerity was low (0.06 cm/sec) and due to net accumulation on the lee-side of the wave. Migration of these bed waves produced horizontal parallel laminae as well as parallel laminae that dipped downstream at low angles (cf. Fig. 14). Similar regular undulatory bed waves in run 33B (Fig. 15) produced no flow separation and represented a stable bed in which grain roughness predominated. Migration was slow and downstream. The wave lengths were 95 ± 10 cm. Lamination was parallel to the bed-surface (Fig. 16) except for minor lenses of cross-lamination where flow separation had evidently occurred.

Neither antidunes nor the sliding bed mode reported by Acaroglu and Graf (1968) were observed. No bed waves were observed to migrate upstream, although it is possible that the bed undulations in run 33B are associated with a pressure wave analogous to a standing wave in open-channel flow. At higher flow intensities than those required for a plane bed, the bed appeared to go through a highly unstable dune-plane phase before being completely eroded, after which all sediment was transported in heterogeneous suspension.

Influence Of Hydraulic Mean Depth

Because of the influence of the pipe walls on velocity distribution in pipe-flow systems, the water depth parameter used is hydraulic mean depth, R, equal to the cross-sectional area of flow divided by the wetted perimeter. With dunes on the bed, the average cross-sectional area occupied by sediment was estimated from the dune profiles measured with the template. Figure 17 shows the relationship between R, pipe diameter, and actual water depth along the centre line of a circular pipe cross-section. It can be seen that R is a

maximum where bed thickness equals 19 per cent of pipe diameter. The width of the sediment bed in such a circular cross-section would be 78 per cent of tunnel diameter.

Relationship to dune height

Hydraulic mean depth varies from 1 to 3 times dune height for all runs, except for 34A and 29B ($\frac{R}{H}$ equals 8.5 and 8.2, respectively) where the gently convex-up bed waves were exceptionally low and appeared to be transitional to a plane bed. The average R/H ratio for the other thirteen cases is 1.6.

Thus it may be possible to use dune height as a guide to water depth in pipe-flow systems, just as can be done for open-channels. With progressive filling up of a circular cross-section with sediment, the actual water depth along the centre line decreases regularly from 4R (no sediment) to 1.5R when 99 per cent of the cross-section is choked off. At maximum R, water depth is 2.7R, and when the tunnel is 50 per cent full of sediment, the water depth along the centre line is 2R. For a non-circular tunnel cross-section that is wide with respect to actual water depth, i.e. the extreme case in deviation of tunnel cross-section from a circle, the wetted perimeter in effect becomes twice channel width and actual water depth would approach 2R. Thus, without making too serious assumptions regarding how much of an idealized cross-section is filled with sediment, or regarding the position of an observation with respect to the highest point in a circular-shaped roof, actual water depth could be calculated to be 2 to 3 times the hydraulic mean depth, R. Thus, as a guide, actual water depth would be about 2 to 10 times dune height.

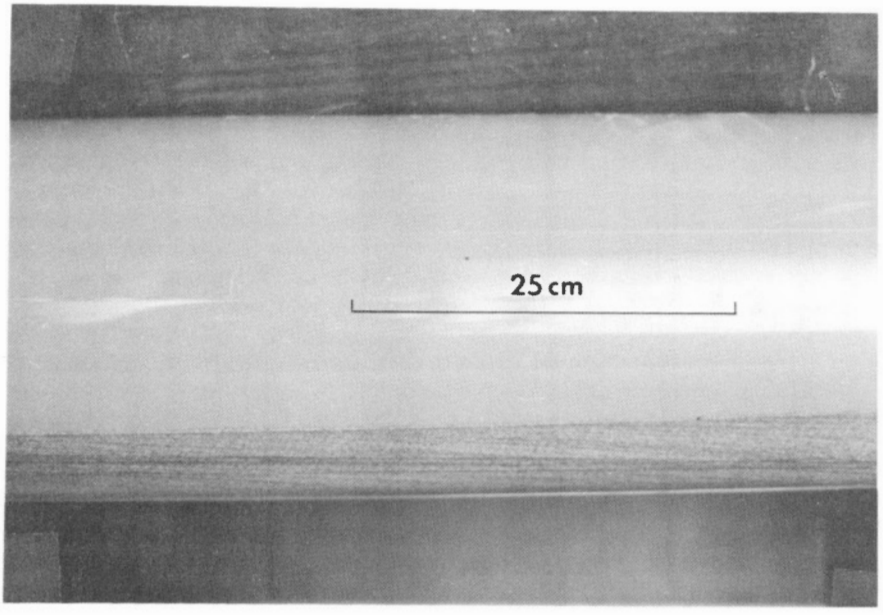

Figure 14. Plane bed after run 24A. Parallel laminations dip gently downstream due to slow migration of low undulatory bed waves at an earlier stage in the run. (GSC photo 159716)

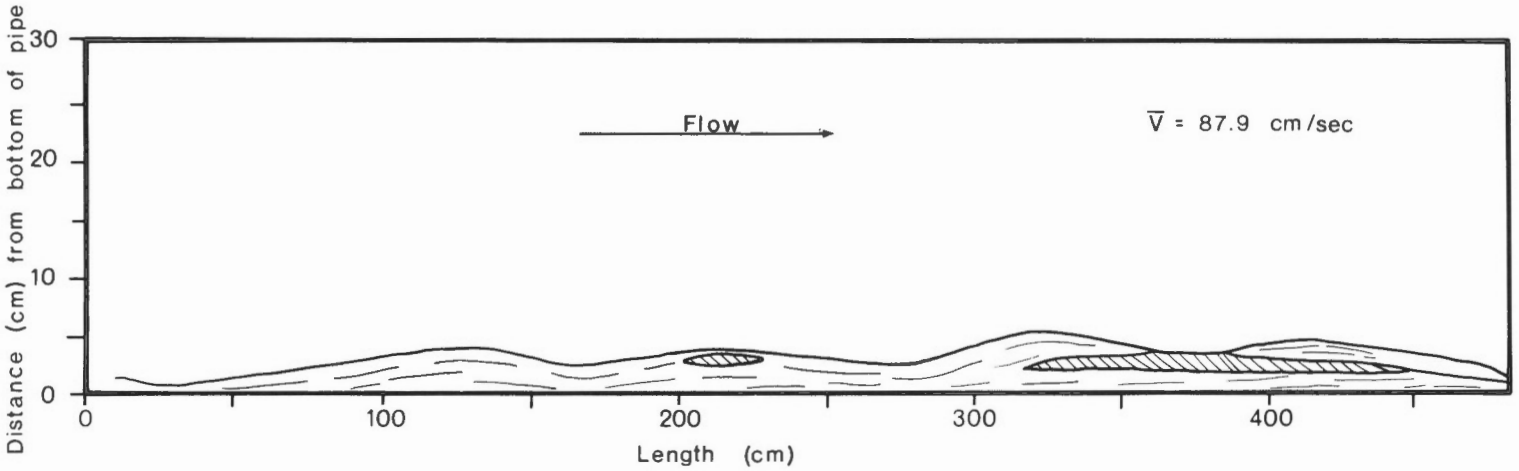

Figure 15. Diagram of undulatory bed and stratigraphy after run 33B. Regular bed waves underlain by laminations parallel to bed surface. Small cross-stratified lenses indicate where zones of flow separation had developed locally. (Fig. 16 from station near 125 cm)

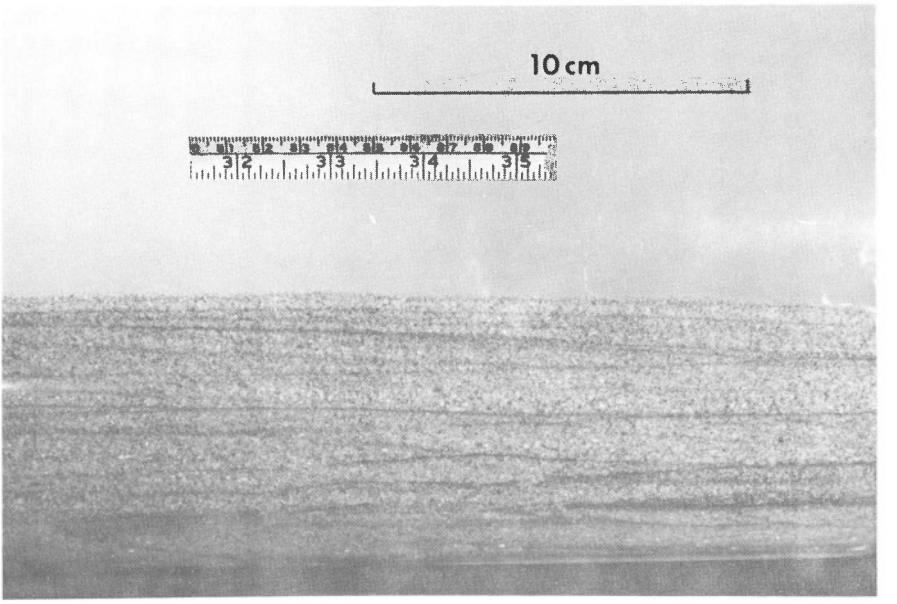

Figure 16. Laminations parallel to gently undulatory bed surface after run 33B. Scale on photo in centimetres and inches. (GSC photo 159725)

Relationship to sediment concentration and bed condition

The maximum limiting value of R, being 0.3044 times pipe diameter, is 7.55 cm for the 24.8-cm pipe and 9.11 cm for the 29.9-cm pipe. As concentration of sediment in transport increases at any given discharge (Fig. 18) there is a tendency for the bed to aggrade in the following manner (see also Fig. 17):

(a) Bed thickness increases with increasing R, the bed being characterized first by dunes and then by dune-plane fluctuations.

(b) Aggradation continues until bed thickness equals about 19 per cent of pipe diameter, i.e. R is at a maximum, and a plane bed is characteristic. The only stable plane bed observed (run 24A) occurred exactly at R = 7.55 cm, the maximum value of R for that pipe. In the 24.8 cm pipe, this threshold appeared to occur at about $\overline{C}_T$ = 1,500 to 2,000 ppm.

(c) As aggradation continues, R is decreased slightly and dunes and dune-plane fluctuations again characterize the bed form. Run 25A at Q = 30.0 litres/sec shows this decreased R value.

It is apparent that for high concentrations of sediment in transport the pipe-flow system tends to maximize the hydraulic mean depth by adjustment of both bed height and bed form. This minimizes the bed shear stress. Continued aggradation in a pipe system with a rigid upper boundary decreases R, increases the shear stress on the bed, and results in high energy loss due to excessive turbulence. This, in turn, generates a highly unstable dune-plane fluctuation of the bed.

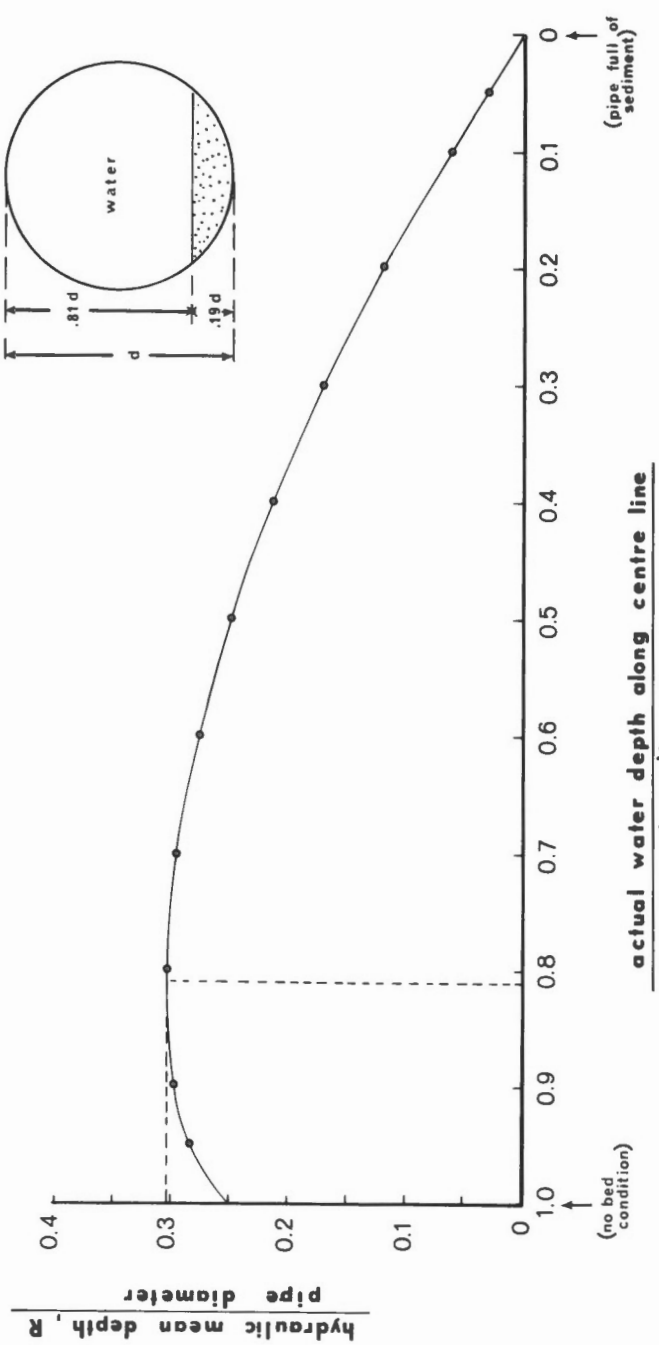

Figure 17. Relationship between R, pipe diameter, and actual water depth along the centre line of a circular pipe cross-section, with pipe flowing full and with a sediment bed. Note that maximum limiting value of R equals 0.3044 x pipe diameter, and is reached when pipe is 19 per cent full of sediment. (From tables in Chow, 1959)

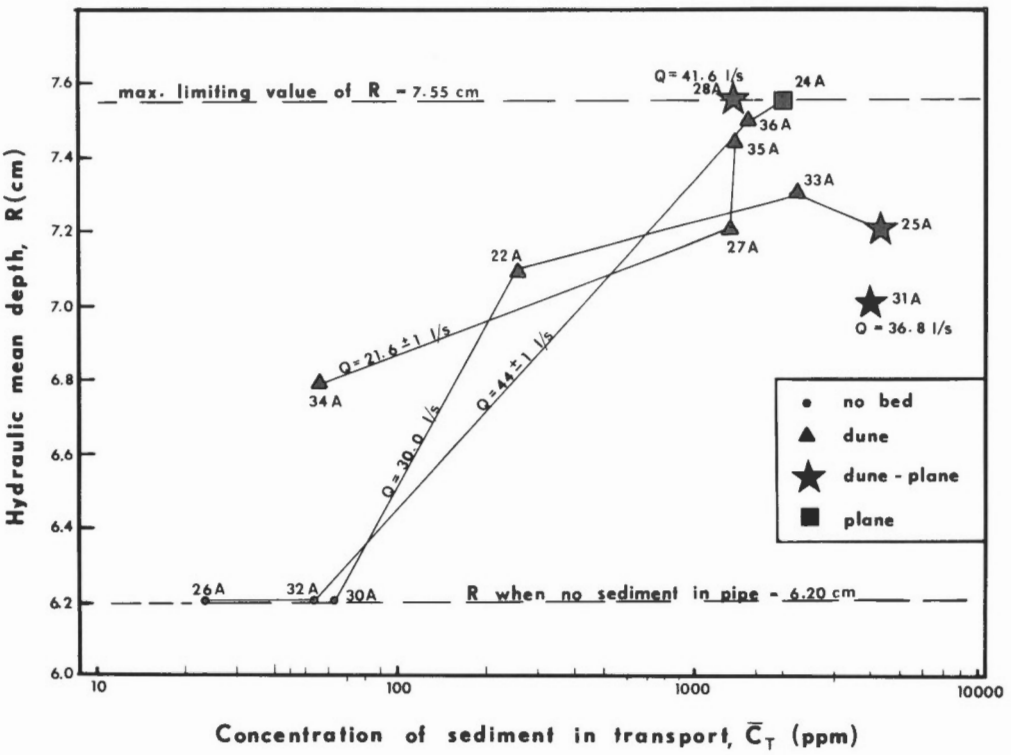

Figure 18. Effect of sediment concentration on hydraulic mean depth at particular discharges in 24.8-cm pipe.

SUMMARY AND POSSIBLE IMPLICATIONS FOR NATURAL SYSTEMS

The objective of the experiment was to gain some insight into conditions of sedimentation in pipe systems and to investigate criteria that might be diagnostic in the field for sediments deposited in natural tunnels flowing full.

Observations from the present pipe-flow experiment that may have a bearing on natural systems can be summarized in two categories:

(a) Primary sedimentary features

(i) Foreset laminations tend to be tangential at the base and become finer grained down the foreslope. Insofar as the size gradation on the foreslope is dependent on the finer grains reaching the foreslope by settling through the zone of flow separation, this "reverse" gradation may be a function of scale of the laboratory dunes, however, dunes of comparable size occur in nature and this feature could be present in natural dunes of this scale;

(ii) "over-building" of the upper part of the foreslope results in a slumping mechanism that produces a slope discontinuity in the upper part of the foreset lamination;

(iii) upward convexity of stoss sides of dunes leads to common occurrences of stoss laminations;

(iv) parallel laminations dipping gently downstream were generated by slow downstream migration of undulatory, regularly spaced low bed waves;

(v) plane beds generated planar laminations parallel to the bed surface; and

(vi) the succession of bed forms with increasing concentration of sediment in transport at a given discharge was: ripple → dune → dune-plane → plane → dune-plane → total suspension. Neither antidune nor sliding-bed modes were observed.

(b) Relationship of bed form to hydraulic parameters

(i) Dune celerity is directly proportional to the cube of mean flow velocity;

(ii) ratio of mean flow velocity to celerity is inversely proportional to the square of the Reynolds Number;

(iii) ripple symmetry index is directly proportional to the square of the Reynolds Number;

(iv) dune height is 1/3 to 1 times hydraulic mean depth; actual water depth is 2 to 10 times dune height; and

(v) the system tends to maximize the hydraulic mean depth by adjustment of both bed height and bed form.

It must be strongly emphasized that quantitative extrapolation of results from this simple experiment to the complexities of a natural system would be, at best, a tenuous exercise. It is probable that irregularities in the boundaries and the difference in scale of a natural subglacial flow system would make the occurrence of particular sedimentary details such as reverse sorting on foresets, rare in nature. However, even occasional observation of such characteristics could prove to be diagnostic. In addition, a system flowing beneath ice may adjust the position of its upper boundary with respect to the bed merely by melting the roof upward (and the walls laterally) with heat energy generated by friction in the system. In a natural glacial system, water discharge and sediment load would be highly variable, calibre of sediment supplied to the system could change abruptly, temperatures would be near 0° C, and ice could interact with the system in many ways. Finally, there can be no net sediment accumulation under true equilibrium conditions.

The best data available on natural concentrations of sediment in subglacial transport come from measurements taken directly at glacier termini. There are few sources that attempt to place numbers on total sediment discharge associated with water discharge. Østrem et al. (1970) give figures for Norwegian glaciers that indicate $\overline{C}_T$ values of 50 to 500 ppm averaged over the entire field season. Within this, there are numerous sediment concentration peaks as much as 300 times the base concentration value. Commonly, much of the sediment is transported in only a small proportion of the run-off time, and concentrations vary greatly in different parts of the day. Thus, sediment concentrations measured in the present experiment are also experienced naturally, although natural concentrations far in excess of 4,000 ppm may be sedimentologically the most important in a natural system. High sediment concentrations would favour deposition in the system.

The senior author has studied in detail sedimentary structures exposed in the Windsor esker, Quebec. This esker was partly deposited in a subglacial tunnel that discharged at a depth of 105 metres into a lake that stood against the glacier terminus. The subglacial tunnel, therefore, had to

have flowed full. Thick sections (>16 m) of sand and gravel in this esker are characterized entirely by parallel bedding and large-scale tabular cross-stratification (sets average 40 cm thick and range up to 120 cm); scour-and-fill structures are not common. It is apparent that sedimentation history was one of essentially constant aggradation. Stoss-laminae of dunes were observed frequently, as were parallel laminations that were both horizontal and gently dipping downstream. Neither the slope discontinuity in the foresets, nor the gradation of coarse to fine material down the foreset were observed. Dunes and plane beds were the stable bed forms and, from experimental results reported here, the inference could be made that the section was deposited at or near maximum hydraulic mean depth. Dune heights of 40 cm may indicate actual water depths of 1 to 4 metres. Constant aggradation of several metres of section under a water depth of 1 to 4 metres and associated with a constantly high bed-shear stress indicates that accumulation was accommodated by an upward melting of the ice roof. Because R was maintained near a maximum as sediment accumulated, excess energy apparently was expended as heat energy by a melting upward of the ice roof, rather than by eroding the bed. There should similarly have been a tendency for the tunnel to widen during phases of sediment accumulation.

Glacier tunnel cross-sections can be directly observed only when they are at least partially occupied by air. Lateral ablation might be expected to predominate over vertical ablation in a tunnel only partly water-filled. Consequently there is uncertainty regarding shape due solely to ablation by meltwater. Stokes (1958) walked several hundred metres in a subglacial tunnel in Norway and provided a particularly good description of tunnel shape. The flat floor was underlain by boulders; the passages were roughly semicircular in cross-section with large polygonal scallops on roof and sides. Only rarely did the height of the roof exceed 3 metres and the width of the floor 10 metres. Small tributary passages were frequently 2 metres wide and one metre high. Koch and Wegener (1911) show several excellent photographs of subglacial tunnels from Greenland and illustrate surveyed cross-sections from a subglacial tunnel system that they followed for 2,000 metres. Tunnel heights above flat, boulder-strewn floors averaged about 5 metres, with a maximum of 15 metres. From these reports, and from numerous reports made informally to the authors, it would seem that a common cross-sectional shape varies from circular to roughly semi-elliptical, with a flat floor and with bed width as much as 5 times greater than channel height. For any given field situation, water depth and channel width should be estimated from dune height, lateral variation of sediment, and dimensions of the sediment ridge (taking side-wall collapse into account).

Once tunnel dimensions are approximated, momentary discharges could be estimated if a measure of water velocity was available. This could possibly be estimated from considerations of particle size and critical tractive force. The relationship of ripple symmetry index to mean flow velocity should be investigated further before being applied to a natural system.

REFERENCES

Acaroglu, E. R., and Graf, W. H.
1968: Sediment transport in conveyance systems - Part 2: The modes of sediment transport and their related bed forms in conveyance systems; Bull. Intern. Assoc. Sci. Hydrol., v. 13, no. 3, p. 123-125.

1969: The effect of bed forms on the hydraulic resistance; Proc. Int. Assoc. Hydrol. Res., 13th Congress, Kyoto, Japan, v. 2, p. 199-202.

Chow, Ven Te
1959: Open-channel hydraulics; McGraw Hill Book Company, Inc., Toronto, 680 p.

Craven, J. P.
1952: The transportation of sand in pipes: I. Full-pipe flow; 5th Hydraulics Conf., Univ. Iowa, Eng. Bull. 34, p. 67-76.

Graf, W. H.
1971: Hydraulics of sediment transport: McGraw Hill Book Company, Inc., Toronto, 513 p.

Koch, I. P., and Wegener, A.
1911: Die glaciologischen beobachtungen der Danmark-expedition; Medd. om Grønland, v. 46, 77 p.

McDonald, B. C.
1972: The Geological Survey of Canada sedimentation flume; Geol. Surv. Can., Paper 71-46, 12 p.

Østrem, G., Ziegler, T., and Ekman, S. R.
1970: Slamtransportundersökelser i Norske Bre-Elver, 1969 (Sediment transport studies at selected glacier streams in Norway, 1969); Norges Vassdrags - Og Elektrisitetsvesen, Hydrologisk Avdeling, Rept. no. 6/70, p. 68 (English summary).

Stokes, J. C.
1958: An esker-like ridge in process of formation, Flatisen, Norway; J. Glaciol., v. 3, p. 286-289.

Tanner, W. F.
1967: Ripple mark indices and their uses; Sedimentology, v. 9, p. 89-104.

Task Committee for Preparation of the Sedimentation Manual
1970: Sediment Transportation Mechanics: Part J. Transportation of Sediments in Pipes; J. Hydraul., Proc. ASCE, v. 7, p. 1503-1538.

Thomas, D. G.
1964: Periodic phenomena observed with spherical particles in horizontal pipes; Science, v. 144, p. 534-536.

United States Inter-Agency Committee on Water Resources
1958: Some fundamentals of particle size analysis: a study of methods used in measurement and analysis of sediment loads in streams; Rept. no. 12, U.S. Govt. Printing Office, 55 p.

EXPLANATION OF SYMBOLS

(bar over symbol indicates mean value)

Symbol	Parameter	Units
a, b, c,	long, intermediate, short grain axes, respectively (referred to in Corey shape factor only)	cm
c	celerity, or rate forward of migration of bed form	cm/sec
C_T	total concentration of sediment in transport (by weight)	ppm
g	acceleration of gravity	980 cm/sec^2
H	height of bed form	cm
Q	discharge	l/sec
R	hydraulic mean depth $= \frac{\text{cross-sectional area of flow}}{\text{wetted perimeter}}$	cm
Re	Reynolds Number $= \frac{\bar{V}\, 4\, R}{\text{kinematic viscosity of water}}$	
RI	ripple index $= \frac{\lambda}{H}$	
RSI	ripple symmetry index $= \frac{\text{stoss length}}{\text{lee length}}$	l/sec
T	temperature	° C
$\bar{V}$	mean flow velocity $= \frac{Q}{\text{cross-sectional area of flow}}$	cm/sec
λ	length of bed form	cm
ω_{50}	median settling velocity in calm water	cm/sec